Available online at www.sciencedirect.com
SCIENCE DIRECT®
Experimental Thermal and Fluid Science 29 (2005) 579–590
Experimental Thermal and Fluid Science
www.elsevier.com/locate/etfs

Pumping criterion and dynamic measurements of an inverted U-shape heat driven pump using microchannels and miniature check valves

J.L. Xu *, X. Shi

Guangzhou Institute of Energy Conversion, Chinese Academy of Sciences, Wushan, No.1 Nengyuan Road, Guangzhou 510640, PR China

Received 20 April 2004; accepted 15 August 2004

Abstract

We demonstrated an inverted U-shape heat driven pump consisting of a microchannel heat sink, two vertical branches and two miniature check valves. A new criterion, which is governed by the fluid physical properties, the geometry effect and the heat transfer rates at various oscillating stages, was developed. The theory can explain the operating range of the applied heating power. The dynamic measurements with a high speed data acquisition system shows that periodically a full cycle can be subdivided into a short liquid suction stage, a bulk boiling and a fluid discharge stage, followed by a pressure decrease stage with both of the valves closed. The average mass flow rate is small and can be computed by the energy conservation equation. The cycle period is shortened with increasing the applied heating power. The wall temperatures of the microchannel heat sink are oscillating with small amplitudes but they are slightly higher than the saturated temperature of the working fluid by several degrees. Deionized water was selected as the working fluid. Finally a closed loop heat driven pump design incorporating the microchannel heat sink and the condenser fin heat sink is proposed.

Keywords: Heat driven pump; Fluid discharge/suction criterion; Oscillating; Thermal performance

1. Introduction

For many years people think about the circulation loop that can pump fluid and dissipate heating power without mechanical moving components such as pumps. Such piece of hardware has the advantages of simple geometry configuration and high reliability. Heat pipe which was invented by Gaugler in 1942 and realized by Grover in 1964, has been found wide applications in power, chemical and electronic cooling engineering [1]. In recent years, due to the high demand of electronic cooling at high heat fluxes, capillary pump loop (CPL) and loop heat pipe (LHP) have also been developed.

As another kind of passive heat transfer device, heat driven pump was first demonstrated by Yamamoto et al. [2,3] using the single U-shape tube with the inside diameter of 11.5 mm and two "big" check valves connected in 1980s. Later Takamura et al. [4,5] studied the heat driven pump at macroscale using a single glass tube as the test section. Some phenomena such as dry-out occurring at higher heating powers were observed, observations performed by the naked eyes were performed for the bubble formation of the pumping cycle. Xu et al. [6,7] reported the study on the U-shape heat driven pump at miniature scale with a single glass tube as the test section which has an inside diameter of 3.0 mm and an effective heating length of 60 mm. The pump dynamics were measured and a full cycle has been divided into a sensible heating, a phase-change with fluid discharge followed by a liquid suction substages. The dynamic vapor–liquid interface in the glass capillary tube was modeled in terms of the moving boundary theory considering the liquid and the vapor–liquid as the dominant regions.

* Corresponding author. Tel./fax: +86 20 87057656.
E-mail address: xujl@ms.giec.ac.cn (J.L. Xu).

0894-1777/$ - see front matter © 2004 Elsevier Inc. All rights reserved.
doi:10.1016/j.expthermflusci.2004.08.004

Nomenclature

A_{fin}	total fin area of the microchannels (m^2)
a_v	sound speed of saturated vapor (m/s)
C_1	non-dimensional parameter defined in Eq. (18)
C_2	non-dimensional parameter defined in Eq. (19)
$C_{P,v}$	specific heat of vapor (J/kg K)
$\frac{dp}{dt}\|_{boil}$	pressure change rate due to boiling in the microchannels (Pa/s)
$\frac{dp}{dt}\|_{con}$	pressure change rate due to condensation in the vertical discharge branch (Pa/s)
$\frac{dp}{dt}\|_{net}$	net pressure change rate balanced by the boiling in the microchannels and the condensation in the vertical discharge branch (Pa/s)
g	gravity acceleration (m/s^2)
Gr_δ	Grashoof number
h_{in}	liquid enthalpy of the inlet beaker (J/kg)
$h_{sat,v}$	saturated vapor enthalpy (J/kg)
K_v	thermal conductivity of the vapor (W/m K)
K_t	thermal conductivity of the capillary tube (W/m K)
m	average circulation flow rate (kg/s or g/h)
m_v	vapor mass (kg)
$Nu_{v,c}$	Nusselt number between the vapor and the microchannel wall surface, natural convection component
p	pressure (Pa)
p_{air}	the environment pressure (Pa)
Pr	Prandtl number
$q_{v,r}$	heat flux due to the radiation heat transfer component between the vapor and the microchannel wall surface (W)
Q	applied heating power (W)
Q_{boil}	boiling heat transfer rate in the microchannels (W)
Q_{con}	condensation heat transfer rate in the discharge branch (W)
$Q_{con,v}$	condensation heat transfer rate for the discharge branch that is exposed in the environment (W)
$Q_{con,b}$	condensation heat transfer rate for the capillary length that is immersed in the outlet beaker (W)
Q_{solid}	part of the applied heating power that is absorbed by the solid material of the microchannel heat sink (W)
Q_v	single-phase vapor heat transfer rate in the microchannels (W)
$Q_{v,c}$	natural convection component of the heat transfer rate between the vapor and the microchannel wall surface (W)
$Q_{v,r}$	radiation heat transfer rate between the vapor and the microchannel wall surface (W)
r	latent heat of evaporation (J/kg)
r_{in}	inner radius of the capillary tube (m)
r_o	outer radius of the capillary tube (m)
R	gas constant (J/kg K)
t	time (s)
T	temperature (°C)
T_{in}	inlet temperature of the microchannels (°C)
T_{out}	outlet temperature of the microchannels (°C)
T_v	vapor temperature (°C)
T_w	wall temperatures (°C)
T_{wo}	outside wall temperature of the capillary tube (°C)
V_M	microchannel volume including the two plenums (m^3)
$V_{v,t}$	volume that is occupied by the vapor in the microchannels and the discharge branch (m^3)
ρ_l	liquid density (kg/m^3)
ρ_v	vapor density (kg/m^3)
ε_v	emissivity of the vapor
α_v	absorptivity of the vapor
$\alpha_{v,c}$	convection heat transfer coefficient between the vapor and the wall surface (W/m^2 K)
β	volume expansion ratio of the vapor (1/K)
v	kinematics viscosity (kg/ms)
δ	the gap of the microchannel (m)
ΔT	temperature difference between the channel wall surface and the fluid (°C)
Δt	a short period of time elapsed over the pressure change rate (s)

In the present paper, we demonstrated an inverted U-shape heat driven pump using microchannels and miniature check valves, which has potential applications for electronic cooling. The pump can suck the liquid from the lower position tank and discharge the fluid to the higher position tank. The pumping process was controlled by fluid expansion in microchannels and condensation in discharge branch, thus it is not affected by gravity. Based on the analysis of the physical mechanism of the pumping process, we presented a new criterion governing the necessary conditions that ensure the function of the device. The measurements of the dynamic pressure, fluid/wall temperatures were performed. It is identified that a full cycle can be subdivided into a very short liquid suction stage followed by a longer fluid discharge stage and a pressure

decrease stage at which both of the two check valves are closed. The pumping process was analyzed with the help of the developed theory and the pumping performance is given.

2. Working principle of the heat driven pump

Fig. 1 shows the schematic diagram of the heat driven pump. The end of the suction branch should be immersed in the liquid tank. The suction/discharge branches were directly exposed in the environment thus heat transfer can take place between the branches and the environment. Contradictory to other passive cooling devices such as loop heat pipes which have the wick structure for the fluid suction branch, it is not necessary to use the wick structure for the liquid suction branch of the heat driven pumps due to the distinct working mechanism of the fluid circulation fully controlled by the boiling and condensation inside. Heat driven pumps do work well without the wick structure of the suction branch. The suction branch was always full of subcooled liquid thus it only functions as the connection tube. However, the heat transfer between the discharge branch and the environment is very important for the pumping process, which is sensitive to the distance between the microchannels and the outlet check valve. If such distance is too short, the device may not function. Therefore the outlet check valve is located at the end of the discharge branch. Initially the loop is full of subcooled liquid without any non-condensable gas. Heating power applied on the microchannel heat sink results in the increased liquid temperature in microchannels to the saturated liquid. The continuous heating causes boiling of the liquid in microchannels, leading to a sharp pressure increase and the open of the outlet check valve. With time evolving, the pressure increase rate due to the single-phase vapor expansion in microchannels is less than the decrease rate due to condensation in the discharge branch. Thus the pressure inside the heat driven pump can have a sharp decrease to initiate the liquid suction through the inlet check valve. Sooner or later, the system will evolve the steady periodic process. Alternatively the microchannels have subcooled liquid, saturated boiling, high mass quality vapor or even slight superheated vapor inside. The discharge branch is always partially or totally full of vapor. The saturated boiling in microchannels and condensation in the discharge branch govern the discharge criterion, while the high mass quality or even slight superheated vapor expansion in microchannels and condensation in the discharge branch give the open criterion of the inlet check valve. Only if the heat driven pump satisfies the two criteria, it does work in the periodic mode. Otherwise it loses its function and will burn out. On the average, the discharged mass should be equal to the suction mass for a full cycle.

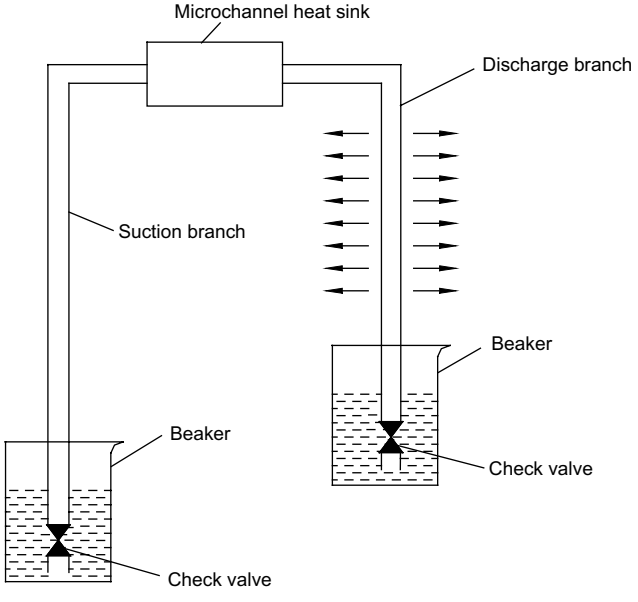

Fig. 1. Schematic diagram of the proposed heat driven pump.

It is well known that microchannels provide large surface to volume ratio. The purpose of using microchannels is to enhance the boiling heat transfer thus shorten the discharge period. Once dry-out occurs in microchannels, the heat transfer coefficient between the wall surface and the vapor is small. The larger surface area of the microchannels can improve the thermal performance at this stage. The present study demonstrates that if the inlet check valve can be activated to suck the liquid, the wall temperatures of the microchannel heat sink are slightly higher than the saturated temperature by several degrees. In other words, the wall temperatures are mainly depended on the saturated temperature of the working fluid. The safety operation of the microchannel heat sink can be guaranteed.

3. Two criteria governing the pumping process

Considering the heat driven pump as an isolated system with both of the two check valves closed. Outside of the two beakers have the environment pressure p_{air}. Boiling in the microchannels results in a very high pressure increase rate versus time. The sharp pressure increase rate integrated over a short period of time $\int_0^{\Delta t} \frac{\mathrm{d}p}{\mathrm{d}t}\mathrm{d}t$ causes a high pressure p inside the heat driven pump. The accumulated pressure inside the loop subtracting the environment pressure actually is the pressure difference over the miniature check valve, which is large enough to overcome the crack pressure of the check valve initiating the fluid discharge. On the other hand, once the high quality vapor occurs in the microchannels, the sharp pressure decrease rate governed by the condensation heat transfer in the vertical discharge

branch can accumulate an apparent negative pressure reference to the environment pressure which is large enough to overcome the crack pressure of the inlet check valve, leading to the liquid suction to the system through the inlet check valve. Based on the above analysis, two criteria were developed, one is for the fluid discharge and the other is for the liquid suction.

3.1. Fluid discharge criterion

Considering saturated liquid in the microchannels, the continuous heating causes boiling heat transfer. The energy conservation equation is written as

$$Q_{\text{boil}}\mathrm{d}t = \mathrm{d}m_{\text{v}} r \tag{1}$$

where Q_{boil} is the boiling heat transfer rate, $\mathrm{d}m_{\text{v}}$ is the mass transferred from liquid to vapor, r is the latent heat of evaporation.

The vapor mass in the heat driven pump has the following relationship with the vapor density:

$$m_{\text{v}} = \rho_{\text{v}} V_{\text{v,t}} \tag{2}$$

where ρ_{v} is the vapor density and $V_{\text{v,t}}$ is the total volume that is occupied by the vapor in the microchannels and the discharge branch.

Differentiating Eq. (2) yields

$$\mathrm{d}m_{\text{v}} = \rho_{\text{v}}\mathrm{d}V_{\text{v,t}} + V_{\text{v,t}}\mathrm{d}\rho_{\text{v}} \tag{3}$$

Because

$$\mathrm{d}V_{\text{l,t}} + \mathrm{d}V_{\text{v,t}} = 0 \tag{4}$$

$$\mathrm{d}V_{\text{v,t}} = \frac{1}{\rho_{\text{l}}}\mathrm{d}m_{\text{v}} \tag{5}$$

Substituting Eqs. (4) and (5) into Eq. (3) yields

$$\left(1 - \frac{\rho_{\text{v}}}{\rho_{\text{l}}}\right)\mathrm{d}m_{\text{v}} = V_{\text{v,t}}\mathrm{d}\rho_{\text{v}} \tag{6}$$

Note that $\rho_{\text{v}}/\rho_{\text{l}} \ll 1$. Combining Eq. (1) with Eq. (6) and applying $a_{\text{v}}^2 = \mathrm{d}p/\mathrm{d}t$, where a_{v} is the sound speed of the saturated vapor, we have

$$\left.\frac{\mathrm{d}p}{\mathrm{d}t}\right|_{\text{boil}} = \frac{a_{\text{v}}^2}{r}\frac{1}{V_{\text{v,t}}}Q_{\text{boil}} \tag{7}$$

Eq. (7) describes the pressure increase rate due to boiling in microchannels.

For the discharge branch, the heat transfer rate Q_{con} is transferred by condensation in the discharge branch, thermal conduction through the solid wall and finally dissipated to the environment by radiation and air natural convection. Similarly, the pressure increase rate can be written as

$$\left.\frac{\mathrm{d}p}{\mathrm{d}t}\right|_{\text{con}} = -\frac{a_{\text{v}}^2}{r}\frac{1}{V_{\text{v,t}}}Q_{\text{con}} \tag{8}$$

Coupling Eq. (7) with Eq. (8), we obtain the net pressure change rate in the heat driven pump as

$$\left.\frac{\mathrm{d}p}{\mathrm{d}t}\right|_{\text{net}} = \frac{a_{\text{v}}^2}{r}\frac{1}{V_{\text{v,t}}}(Q_{\text{boil}} - Q_{\text{con}}) \tag{9}$$

Eq. (9) describes the pressure change rate balanced by boiling in the microchannels and condensation in the discharge branch. In order to ensure that fluid can be discharged, the net pressure change rate by Eq. (9) should be positive thus the pressure can be increased to the crack pressure that can initiate the open of the outlet check valve. Thus the fluid discharge criterion is defined as

$$\left.\frac{\mathrm{d}p}{\mathrm{d}t}\right|_{\text{net}} = \frac{a_{\text{v}}^2}{r}\frac{1}{V_{\text{v,t}}}(Q_{\text{boil}} - Q_{\text{con}}) > 0 \tag{10}$$

3.2. Liquid suction criterion

The liquid suction is possible if the microchannels are occupied by the high quality wet vapor or slightly superheated vapor. Under such condition, the pressure increase rate by single-phase vapor expansion in microchannels may be smaller than the pressure decrease rate due to condensation in the discharge branch. Otherwise the liquid can not be sucked. Assuming the two valves are closed and the saturated vapor exists in the microchannels, at this stage the applied heating power can be divided into two parts: one part is used for the enthalpy increment of the single-phase vapor (Q_{v}) while the other part is for the enthalpy increment of the solid material of the microchannel heat sink (Q_{solid}).

$$Q = Q_{\text{v}} + Q_{\text{solid}} \tag{11}$$

The energy conservation equation for the vapor yields

$$Q_{\text{v}}\mathrm{d}t = \rho_{\text{v}} V_{\text{M}} C_{\text{P,v}}\mathrm{d}T \tag{12}$$

where V_{M} is the microchannel volume occupied by the fluid, $C_{\text{P,v}}$ is the specific heat of the vapor. $\mathrm{d}t$ and $\mathrm{d}T$ are the time and temperature increments respectively.

Assuming vapor as the ideal gas, then

$$p_{\text{v}} = \rho_{\text{v}} R T \tag{13}$$

where R is the gas constant and T is the vapor temperature. Assuming ρ_{v} is constant in the microchannels (constant vapor mass occupied in the microchannel volume), differentiating Eq. (13) and combining with Eq. (12) gives

$$\left.\frac{\mathrm{d}p}{\mathrm{d}t}\right|_{\text{v}} = \frac{R}{C_{\text{P,v}}}\frac{1}{V_{\text{M}}}Q_{\text{v}} \tag{14}$$

Eq. (14) is the pressure increase rate due to the single-phase vapor expansion in the microchannels.

Coupling with the pressure change rate due to condensation in the discharge branch, the net pressure change rate is

$$\left.\frac{dp}{dt}\right|_{net} = \frac{R}{C_{P,v}}\frac{1}{V_M}Q_v - \frac{a_v^2}{r}\frac{1}{V_{v,t}}Q_{con} \quad (15)$$

In order to ensure that the inlet check valve can be opened, the net pressure change rate by Eq. (15) should be negative thus the pressure can be decreased. The liquid suction criterion is written as

$$\left.\frac{dp}{dt}\right|_{net} = \frac{R}{C_{P,v}}\frac{1}{V_M}Q_v - \frac{a_v^2}{r}\frac{1}{V_{v,total}}Q_{con} < 0 \quad (16)$$

3.3. Discussion of the fluid discharge and liquid suction criteria

Actually the fluid discharge criterion by Eq. (10) and the liquid suction criterion by Eq. (16) can be combined as

$$\frac{a_v^2}{r}\frac{1}{V_{v,t}}Q_{boil} > \frac{a_v^2}{r}\frac{1}{V_{v,t}}Q_{con} > \frac{R}{C_{P,v}}\frac{1}{V_M}Q_v \quad (17)$$

Defining the following non-dimension parameters as

$$C_1 = \frac{rR}{a_v^2 C_{P,v}} \quad (18)$$

$$C_2 = \frac{V_{v,t}}{V_M} \quad (19)$$

Eq. (17) can be rewritten as

$$Q_{boil} > Q_{con} > C_1 C_2 Q_v \quad (20)$$

In order to successfully design a heat driven pump, both criteria of fluid discharge and liquid suction should be satisfied. The combined criterion given in Eq. (20) depends on the coefficients C_1, C_2, heat transfer rate Q_{boil}, Q_{con}, and Q_v, where C_1 represents the fluid physical properties, C_2 mainly reflects the geometry effect. The fluid discharge criterion $Q_{boil} > Q_{con}$ indicates that the boiling heat transfer rate in the microchannels should be greater than the condensation value in the discharge branch thus the pressure can be accumulated inside to activate the open of the outlet check valve. However, the heat transfer rate due to the single-phase vapor Q_v in the microchannels should be smaller than the condensation heat transfer rate Q_{con} by $1/C_1C_2$ times, thus the pressure can be decreased to activate the open of the inlet check valve.

4. Experimental study of the inverted U-shape heat driven pump

4.1. Experimental setup of the heat driven pump

Fig. 2 shows the experimental setup of the heat driven pump, consisting of the heat driven pump assembly, the heating power supply unit, the high speed data acquisition system, and the electronic scale for the discharged mass measurement. The heat driven pump is made of two miniature check valves, two soft plastic tubes for the suction and discharge branches and the microchannel heat sink. A 30 μm filter was located in the suction branch to prevent any solid particles entering microchannels. Because the mass flow rate is very small, the gravity pressure drop contributes the major part. Thus arranging the filter in the suction branch has little influence on the pumping process. The two plastic tubes were tightly fitted with the inlet/outlet connection copper tubes of the microchannels. The two soft plastic tubes having 3 mm inside diameter with 1 mm wall thickness were exposed directly in the environment thus condensation heat transfer rate can be finally dissipated to the environment by radiation and air natural convection for the discharge branch. Visualization can also be performed by the naked eyes through the plastic tubes. The two miniature check valves were installed at the end of the two plastic tubes. Two large beakers were used as the liquid tanks, where the two check valves were put inside respectively. The liquid in the inlet beaker was controlled by a PID temperature control unit (not shown in Fig. 2) to keep the constant temperature of 50 ± 0.5 °C. Cold liquid was also deposited in the outlet beaker thus once vapor was discharged into the tank, it is quickly condensed into liquid before any bubble escaped out of the liquid surface. Generally the liquid temperature of the outlet beaker is kept below 40 °C. If the temperature of the outlet beaker is increased to be higher, the "hot" liquid was replaced by the cold one. For all the cases tested, the liquid surface locations of the two beakers were kept constant. The vertical distance between the liquid surface of the inlet beaker and the centerline of the microchannels is 560 mm, such distance becomes 520 mm for the outlet beaker. Thus the liquid surface of the inlet beaker was lower than that of the outlet one by 40 mm.

The power supply unit includes an AC voltage stabilizer, a variac and a powermeter. By adjusting the variac, one can obtain a stable voltage output in the range of 2–220 V resulting in the controlled adjustable heating power in the range of 1–200 W. The precision powermeter measures voltage, current and heating power simultaneously, with the uncertainty of 0.5% in the present test range.

A high speed data acquisition system (DL750, Yokogawa Inc., Japan) with sixteen channels was applied to detect the periodic process. The data sampling rate can be up to 100 K samples per second. For the present applications, the sampling rate is selected as 200/s, which is fast enough to trace the cycle behavior.

The inlet/outlet fluid temperatures were measured by the K-type jacket thermocouples which were located in the inlet/outlet connection tubes of the microchannels.

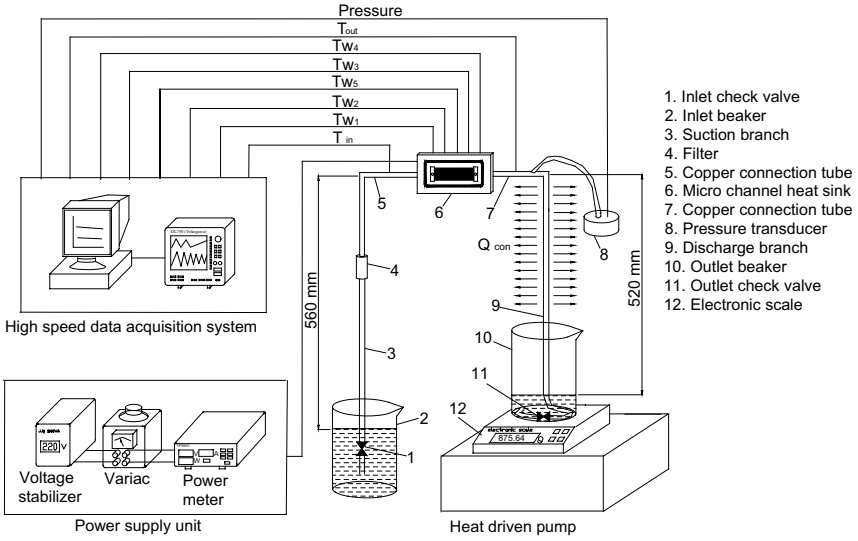

Fig. 2. Experimental setup of the heat driven pump.

The distance between the inlet thermocouple and the inlet plenum of the microchannel is 30 mm. The two thermocouples were located symmetrically about the microchannels. These thermocouples have the measurement errors less than 0.2 °C after calibration with a constant temperature bath. The thermocouples which were arranged in the microchannel heat sink will be described in the next section. The fluid pressure was measured by a precision Setra pressure transducer (Model 206), which was calibrated against a known standard and the uncertainty was less than 0.1%.

The outlet liquid tank was measured by a precision electronic scale, with the uncertainty of 0.01 g. Because the circulation flow rate is very small, the heat driven pump was running at each heating power for more than one hour after the steady oscillating state is reached. The flow rate is obtained by the weight increment over a given long period of time such as 1 h.

The two miniature check valves were provided by Cole-Parmer International USA (U98553-20), having the inside diameter of 1/8 in. (3.175 mm). The crack pressure, at which the valve begins to be opened, is measured to be around 300 mm H_2O. Both of the two check valves were selected to have the nearly same parameters such as crack pressures. Once the pressure drop over a check valve reaches the crack pressure, the valve is open until this pressure drop is decreased to zero.

4.2. Microchannel heat sink

Fig. 3 illustrates the technical detail of the microchannel heat sink, consisting of the pyrex glass cover, the copper frame and the copper block. The deep microchannels were machined in the body of the copper block by the electronic discharge method (EDM). The width of the channel 300 μm and the depth of the channel is 800 μm with the uncertainty of 5 μm. The distance between the neighboring channels is also 300 μm, the planform (top) area is 50×15.3 mm^2 (26 parallel microchannels included). Below the heat sink top surface, four K-type thermocouples (marked from T_{w1} to T_{w4}) were inserted in the 0.8 mm diameter holes along the centerplane to measure the heat sink's stream-wise temperature distribution by bounding with the holes using the high thermal conductivity epoxy containing boron nitride. The fifth thermocouple T_{w5} was arranged just below the thermocouple T_{w2} by a vertical distance of 6 mm. The five thermocouples were made from a single long thermocouple wires. Thus they have the exact same material and the exact same calibration results demonstrating the errors less than 0.2 °C. When these thermocouples are used to measure the wall temperatures, the errors of the relative temperature differences between any two temperatures are reduced due to using the exact same material of the thermocouple wires and the same filling techniques with the holes. Each thermocouple has the axial distance of 10.0 mm and they are symmetric about the microchannel heat sink. The vertical distance between the planform (top) surface and the four thermocouple plane is also 10.0 mm. The total height of the copper block is 35 mm. The distance between the planform (top) surface to the centerline of the larger diameter hole having the inside diameter of 8.0 mm where a cartridge heater was inserted is 26 mm.

At the planform (top) surface of the copper frame, a rectangular O-ring slot was machined. After the fabrication of each pieces, the copper frame and the copper block was bounded by the thermal squeezing method on the standard plane surface. Then the pyrex cover plate and the copper frame was bolted using the screw. The microchannel test module was tested to sustain

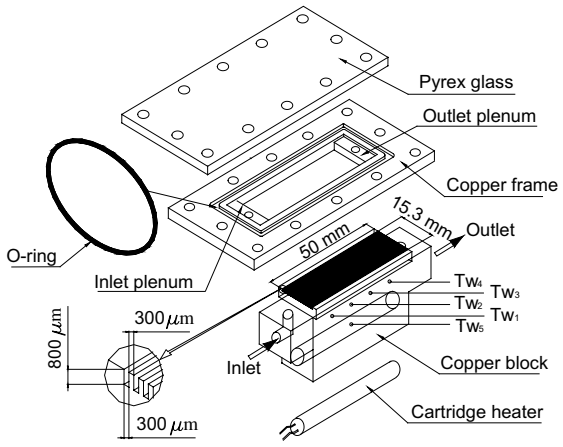

Fig. 3. Three-dimensional view of the microchannel heat sink.

5.0 bar pressure without any leakage for four hours. The axial flow direction of the microchannel is horizontal while the planform (top) surface of the microchannel was vertically arranged, thus the flow visualization can be easily performed with the help of a microscope.

The microchannel heat sink was well insulated using the high quality thermal insulation material except the pyrex glass cover.

4.3. Determination of C_1, C_2, Q_{boil}, Q_v, and Q_{con}

In order to use the two criteria explaining the operating range of the heat driven pump, the parameters of C_1, C_2, Q_{boil}, Q_{v} and Q_{con} should be determined. Among them C_1 and C_2 are the geometry parameters. The physical properties of saturated water and vapor at 1 atm are summarized in Table 1. Considering the discharge branch with the inside diameter of 3 mm and the length of 600 mm, V_{T2} is 4.24 ml. The volume of microchannels including the two plenums V_{M} is 0.852 ml. Therefore

$$V_{\text{v,t}} = V_{\text{M}} + V_{\text{T2}} = 5.09\ \text{ml} \tag{21}$$

$$C_2 = \frac{V_{\text{v,t}}}{V_{\text{M}}} = 5.974 \tag{22}$$

The discharge criterion $Q_{\text{boil}} > Q_{\text{con}}$ is for the low heating power while the suction criterion $Q_{\text{con}} > C_1C_2Q_{\text{v}}$ is for the high heating power, thus these parameters can be evaluated at the different heating power range and they occur at the specific substages. In all the situations, in one full cycle before the liquid is sucked, the microchannels have higher temperatures due to the small heat transfer coefficient between the wall surface and the vapor. Once the nearly saturated liquid is sucked into the system, the suction process is finished quickly, the bulk boiling takes place. The microchannel temperatures will be sharply decreased. Thus the boiling heat transfer rate should be larger than the applied heating power due to the transient heat transfer of the copper block from higher temperature to lower temperature.

When the bulk boiling process finished, the saturated vapor exists in the microchannels, the continuous heating results in the superheated vapor inside. The heat transfer rate Q_{v} between the channel wall surface and the vapor is coming from two parts, one is from the natural convection heat transfer rate $Q_{\text{v,c}}$, the other is the radiation heat transfer rate $Q_{\text{v,r}}$. Also in terms of our present measurements, the maximum wall temperature difference between the channel wall and the saturated fluid is less than 10 °C. Thus the average temperature difference between the wall surface and the fluid ΔT is set as 5 °C. Using the natural convection heat transfer correlation for the rectangular gap [8], the Nusselt number $Nu_{\text{v,c}}$ is given as

$$Nu_{\text{v,c}} = 0.212(Gr_\delta Pr)^{0.25} \tag{23}$$

where Gr_δ is

$$Gr_\delta = \frac{g\beta\Delta T\delta^3}{v^2} \tag{24}$$

$$\alpha_{\text{v,c}} = \frac{Nu \cdot K_{\text{v}}}{\delta} \tag{25}$$

In Eqs. (23)–(25), Gr_δ is the Grashoof number, Pr is the Prandtl number, g is the gravity acceleration, β is the volume expansion ratio, ΔT is the temperature difference between the wall surface and the fluid, δ is the gap of the rectangular channel, v is the kinematics viscosity, K_{v} is the thermal conductivity of the vapor. Substituting $g = 9.81\ \text{m/s}^2$, $\Delta T = 5\ ^\circ\text{C}$, $\delta = 0.3 \times 10^{-3}\ \text{m}$, $\beta = 1/373\ \text{K}^{-1}$, $v = 2.012 \times 10^{-5}\ \text{m}^2/\text{s}$, $K = 2.48 \times 10^{-2}\ \text{W/(m K)}$ into Eqs. (23)–(25) results in $\alpha_{\text{v,c}} = 40.6\ \text{W/(m}^2\ \text{K)}$.

Also based on [8], the heat flux due to the radiation heat transfer component between the channel wall and the vapor can be written as

$$q_{\text{v,r}} = 5.67\left[\alpha_{\text{v}}\left(\frac{T_{\text{w}}}{100}\right)^4 - \varepsilon_{\text{v}}\left(\frac{T_{\text{v}}}{100}\right)^4\right] \tag{26}$$

where ε_{v} and α_{v} are the emissivity and absorptivity of the vapor, respectively. α_{v} has the following relationship with ε_{v}:

$$\alpha_{\text{v}} = \varepsilon_{\text{v}}\left(\frac{T_{\text{v}}}{T_{\text{w}}}\right)^{0.45} \tag{27}$$

In terms of the geometry coefficient, ε_{v} is chosen as 0.2, $q_{\text{v,r}}$ is computed as $21.62\ \text{W/m}^2$. Therefore the total heat transfer rate is

$$Q_{\text{v}} = \alpha_{\text{v,c}}A_{\text{fin}}\Delta T + q_{\text{v,r}}A_{\text{fin}} = 0.55\ \text{W} \tag{28}$$

Table 1
Physical properties of saturated water and vapor at 1 atm

r (J/kg)	$C_{\text{P,v}}$ (J/kg K)	a_{v} (m/s)	R (J/kg K)	C_1
2256.6×10^3	2028.1	340	454	4.37

The condensation heat transfer rate Q_{con} consists of two parts, one is the heat transfer rate for the vertical discharge branch that is exposed in the environment $Q_{con,v}$, the other is the heat transfer rate for the capillary tube immersed in the outlet beaker $Q_{con,b}$.

$$Q_{con} = Q_{con,v} + Q_{con,b} \tag{29}$$

The saturated temperature of the vapor inside the discharge branch is 98 °C corresponding to the local environment pressure. The measured temperature of the outer wall surface of the discharge branch on which the thermocouple wires are attached is 90 °C. Thus $Q_{con,v}$ can be computed using the one-dimensional heat conduction equation for the cylinder as

$$Q_{con,v} = \frac{2\pi K_t (T_v - T_{wo})}{\ln(r_o/r_{in})} \tag{30}$$

where K_t is the thermal conductivity of the capillary tube, T_{wo} is the temperature of the outer wall surface, r_o and r_{in} are the outer and inside radius of the capillary tube. Eq. (30) is correct with the assumption that the temperature of the inside wall surface has little difference with that of vapor inside due to the small inside thermal resistance. Eq. (29) results in $Q_{con,v} = 5$.

It is difficult to determine $Q_{con,b}$. However, an alternative simple method is helpful for such estimation. Arranging a part of the capillary tube in an insulated small beaker instead of the larger one in which the cold liquid is deposited and measuring the temperature increment of the liquid inside the beaker over a given period of time yields $Q_{con,b}$ to be 10 W. With such arrangement the outlet check valve discharges the fluid to the environment directly. The length of the capillary tube that is immersed in the smaller beaker is exact the same as that is put inside the larger outlet beaker initially. Thus the above procedure results in the total condensation heat transfer rate Q_{con} as 15 W.

5. Experimental results and discussion

5.1. Description of the observed flow and boiling phenomenon

When a low heating power such as less than 15 W is applied on the microchannel heat sink, the heat driven pump displays the very slow response. The observations by the naked eyes show that the whole loop including the microchannels and the two vertical branches are full of liquid. Such condition lasts until the bulk boiling process is initiated in the microchannels. The expanded vapor enters the discharge branch. However, because the condensation heat transfer rate in the discharge branch is relative large, little vapor is accumulated there. Much vapor is produced in the microchannels until the superheated vapor appears and the wall temperatures of the microchannel heat sink is increased. Once the microchannel heat sink reaches the temperature of 150 °C, the heating power is turned off manually.

When the heating power is increased larger than 15 W, the normal dynamic operating mode can be established. The heat driven pump repeats the cycle behavior. The vertical suction branch is always full of liquid while the vertical discharge branch is full of bubble slugs separated by the liquid bridge between the two bubble slugs. However, in one full cycle the microchannels evolve the sensible liquid heating, the quick bulk boiling and the high quality evaporating even superheated vapor stages. Once the bulk boiling is suddenly activated, the pressure has a sharp increase. The dispersed bubbles and the bubble slugs are observed during the bulk boiling process. The microchannel heat sink evolves the high quality evaporating process after the short bulk boiling process. The microchannels are full of vapor and the glass cover becomes misty. The temperatures of the microchannel heat sink have a slight increase versus time. The condensation heat transfer in the vertical discharge branch decrease the pressure. Suddenly the cold liquid flushes the microchannels and sweeps all the vapor inside and a new cycle starts.

5.2. Operation range of the applied heating power and compared with the developed theory

The heat driven pump is measured to have an operating range of the heating power. It does operates well with the range of 15 W to 80 W. Below the heating power of 15 W, because the capacity of the condensation heat transfer rate for the discharge branch is relative large, the pressure can not be effectively accumulated inside thus the fluid discharge can not be functioned. While at the extremely high heating powers, the vapor expansion effect is so strong that the negative pressure is difficult to be established thus the liquid suction is not initiated.

Based on the fluid discharge criterion, the lower heating power limit should be larger than the capacity of the condensation heat transfer rate of the discharge branch (including the length that is immersed in the outlet beaker), which is 15 W obtained in the Section 4.3. Such value is consistent with the direct measured lower heating power limit of 15 W.

Also for the liquid suction criterion, coupling $C_1 = 4.37$, $C_2 = 5.974$ and $Q_v = 0.55$ W, leads to $C_1C_2Q_v = 14.4$ W, which is approaching the total condensation heat transfer rate of 15 W. Further increasing the applied heating power such as 80 W, the liquid suction criterion $Q_{con} > C_1C_2Q_v$ is not satisfied. Thus the liquid suction can not be performed. Based on the above description, the present pumping criteria can be effective to explain the operating heating power range phenomenon.

Similarly, the experimental findings in our previous paper [6,7] demonstrate that for a given heat driven

pump with a certain working fluid, there are a minimum heating power and a maximum heating power. Such phenomenon can also be explained by the present theory.

5.3. Pumping cycle measurements and analysis

The high speed data acquisition system recorded the steady thermal/fluid oscillations for each heating power, where pressure is the value referenced to the environment. The pumping cycle characteristics were analyzed with the help of the developed theory. Fig. 4a and b illustrate such transients at the heating power of 40 W. The measured average discharge flow rate is 56 g/h and the cycle period is nearly 20 s. It is seen that all the parameters repeats the process at the same cycle period. The heat driven pump behaves the long period/large amplitude oscillations. However, all the wall temperatures are oscillating with small amplitudes, for instance, T_{w1} is oscillating from 104 °C to 105 °C. We focus a typical full cycle starts from $t = t_B$ to $t = t_E$, referenced as the current cycle. The marked current cycle is followed by the previous one. The later stage of the previous cycle is from $t = t_A$ to $t = t_B$. In order to get better understanding of the oscillating behavior, the following stages are analyzed.

5.3.1. Pressure decrease stage ($t_A < t < {}_B$, previous cycle)

It is observed that at this stage, the high quality vapor exists in the microchannels. With time approaching t_B, the microchannels are totally dried out. With $Q = 40$ W, $m = 56$ g/h and $T_{in} = 50.0$ °C, the simple energy equation yields the outlet superheated vapor temperature which is a couple of degrees higher than the saturated temperature. Both of the two check valves are closed. The thermal/fluid parameters display the following transients. (1) The measured pressure, which is balanced by the vapor expansion in the microchannels and the condensation in the discharge branch, is decreased versus time at the measured pressure decrease rate of 69 286 Pa/s, roughly consistent with the pressure decrease rate of 57 566 Pa/s given in Eq. (16). (2) The inlet and the outlet fluid temperatures are slightly decreased due to the inlet/outlet connection tubes were directly exposed in the environment. (3) The wall temperatures were slightly increased due to the smaller heat transfer coefficient between the wall surface of the microchannels and the vapor. Major part of the applied heating power is converted to the enthalpy increment of the solid copper block.

5.3.2. Liquid suction stage ($t_B < t < t_C$, current cycle)

Once the pressure is decreased to activate the open of the inlet check valve at $t = t_B$, the cold liquid is sucked into the system. The vapor in the microchannels is quickly collapsed by the invading liquid. Then the microchannels including the inlet/outlet plenums are full of liquid. The thermal/fluid parameters have the following

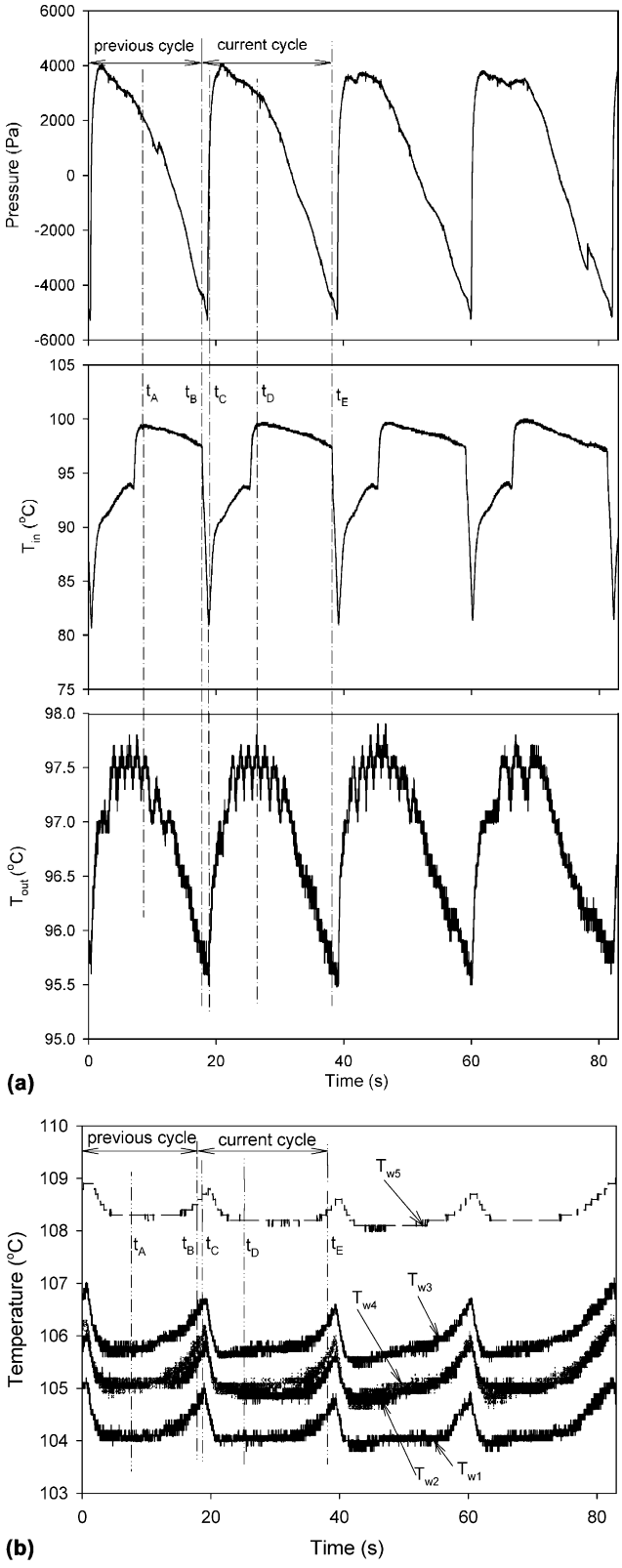

Fig. 4. (a) Recordings of pressure and inlet/outlet fluid temperatures; (b) recordings of wall temperatures of the microchannel heat sink at $Q = 40$ W.

characteristics. (1) The pressure continues to be decreased until the minimum point is reached at $t = t_C$. (2) The inlet temperature has a sharp decrease. (3) The inlet/outlet temperatures have minimum points at $t = t_C$. (3) The wall temperatures still increase due to the thermal inertia of the copper block. However, following $t > t_C$, they are sharply decreased, indicating the microchannels are well cooled after the liquid suction. The suction stage lasts only one second starting from $t = t_B$ and ending at $t = t_C$.

5.3.3. Boiling and discharge stage ($t_C < t < t_D$, current cycle)

Even though the inlet liquid tank is kept as 50 °C, the inlet/outlet thermocouples always detect higher temperatures, which is caused by the axial heat conduction between the heated copper microchannel heat sink and the connection tube on which the inlet/outlet thermocouples were located. It is shown in Fig. 4a that the minimum inlet liquid temperature is about 80 °C. Once the cold liquid enters the microchannels, it is quickly warmed up to the saturated liquid due to the heat received from the microchannel heat sink and the condensed vapor previously existed in the microchannels.

After the very short period of heating up process, bulk boiling takes place in the microchannels and induces a very steep pressure increase synchronously, leading to the open of the outlet check valve thus the fluid discharge begins. The outlet thermocouple detects the expanded vapor and is increased from 95.5 °C to 97.5 °C. Therefore the fluid discharge starts from $t = t_C$ and ends at $t = t_D$. The inlet/outlet temperatures have maximum values at $t = t_D$.

In the earlier stage of this period, the pressure has a very steep increase. However, once the fluid discharge begins, the pressure is decreased. It is also identified that the time of the fluid discharge is much longer than that of the liquid suction.

5.3.4. Pressure decrease stage ($t_D < t < t_E$, current cycle)

This stage repeats the process for $t_A < t < t_B$ in the previous cycle, which has been described. Both of the two check valves are closed. The microchannels evolve the high quality vapor dry-out and the slight single-phase superheated vapor heat transfer. The pressure decrease is contributed from the condensation heat transfer in the discharge branch.

From Fig. 4b it is shown that the wall temperatures are increased along the flow direction ($T_{w1} < T_{w2} < T_{w3}$), but the difference between the minimum and the maximum is about 2 °C. The temperature difference between T_{w5} and T_{w2} is 3.3 °C. Assuming the linear distribution of the wall temperatures in the vertical coordinate of the copper block, the bottom wall temperature is 101 °C, which is 3 degrees higher than the saturated temperature of 98 °C corresponding to the environment pressure. All the wall temperatures are oscillating in the trapezoid form, with small oscillation amplitudes.

Similar transient measurements are demonstrated in Fig. 5a and b at the heating power of 60 W. Again it is seen that these parameters are repeating periodically. The average mass flow rate is 85 g/h, which is higher than that at 40 W. The cycle period is 15 s, which is shorter than that at 40 W. From Fig. 5b it is shown that due to the higher heating power, the wall temperatures are oscillating in the triangular form instead of the trapezoid form at 40 W. All the wall temperatures are higher by 2–3 degrees than those at the heating power of 40 W. For all the heating power tested, the wall temperatures are slightly higher than the saturated temperature of the working fluid by several degrees.

5.4. Pumping performance

Fig. 6 shows the average flow rates and the cycle periods for the present heating power range. The pumping flow rates are increased linearly with increasing the applied heating power. From the energy conservation point of view, for each cycle, the subcooled liquid in the inlet tank should be pumped into the microchannels and attains the slight superheated vapor condition with the mass flow rate of m and the heating power of Q, thus the mass flow rate can be calculated using the following equation:

$$Q = m(h_{sat,v} - h_{in}) \tag{31}$$

Neglecting the small enthalpy increment from the saturated vapor to the very slight superheated vapor causes the errors less than 6% of the mass flow rate.

The cycle periods are decreased with increasing the heating power, which is caused by the increased pressure change rates relating to the boiling heat transfer rate, the single-phase vapor heat transfer rate in the microchannels and the condensation heat transfer rate in the discharge branch.

6. Practical significance/usefulness

Even though the concept of heat driven pumps at macroscale was presented in 1980s [2,3] and the improvement was reported in 1995, 1998 [4,5], real applications of heat driven pumps for the electronic cooling was not found, to the author's knowledge. Dissipating high heat flux electronic cooling device not only requires an effective microchannel or porous medium heat sink, but also a powerful pumping equipment to circulate the flow rate around the loop. Forced convective liquid/two-phase microchannel heat sinks need a pump with a mechanical moving component which

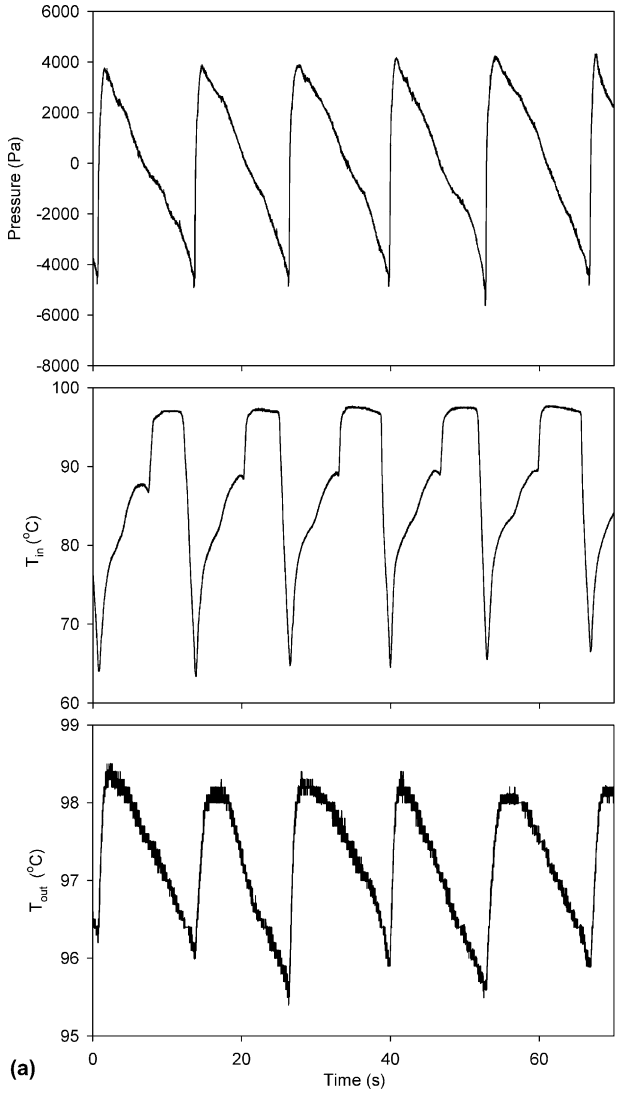

Fig. 5. (a) Recordings of pressure and fluid inlet/outlet temperatures at $Q = 60$ W; (b) recordings of wall temperatures of the microchannel heat sink at $Q = 60$ W.

definitely increases the facility complicacy and the noise. Passive electronic cooling device has the advantages such as simple geometry configuration and high reliability. Due to the boiling and condensation heat transfer dominated in the heat driven pump, gravity force has less effect. Thus it can be used as a kind of passive

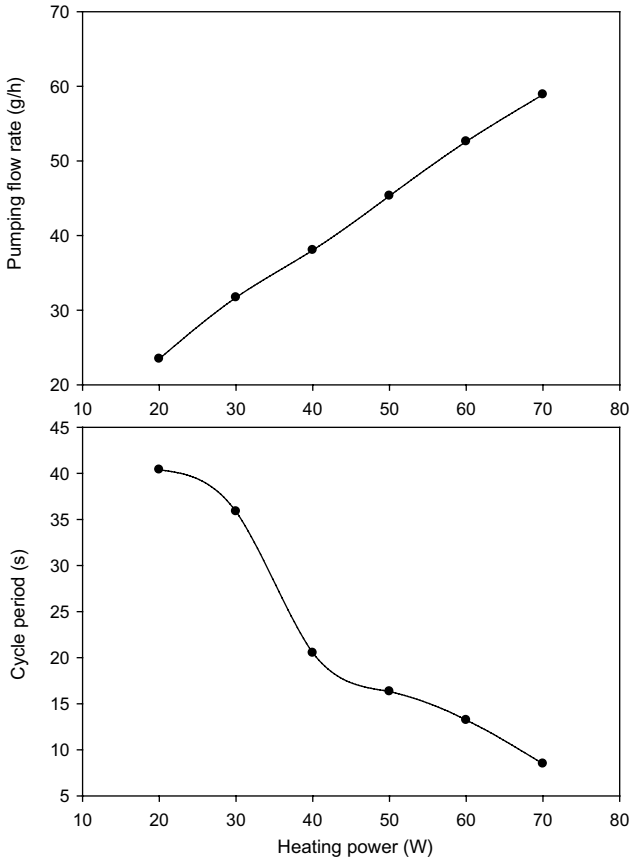

Fig. 6. Pumping flow rate and cycle period versus heating power.

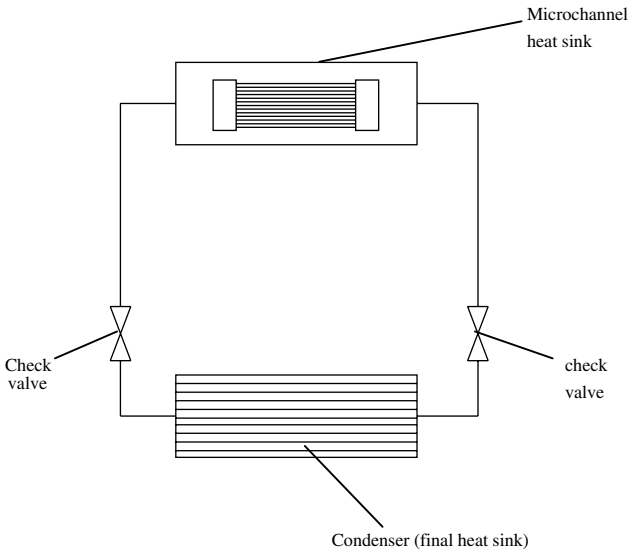

Fig. 7. Proposed closed loop heat driven pump design using microchannels and miniature check valves.

cooling device. Also the heat receiving piece can be located above the heat dissipating piece.

Further improvement of the heat driven pump will replace the two beakers by a fin heat sink condenser, in which the discharged hot fluid is condensed into cold liquid. Heat received by the microchannels is finally dissipated to the environment by the fin heat sink condenser. Fig. 7 shows the proposed closed loop heat driven pump. Vacuum the closed loop initially and then charge the loop with a certain quantity of liquid, the flow rate will be created automatically once heating is applied on the microchannels.

7. Conclusions

An inverted U-shape heat driven pump was developed. The device has no mechanical moving components with simple geometry configurations, which can pump fluid from lower position to higher position and dissipate heating power. It is controlled by fluid expansion and condensation thus gravity force has no effect. In terms of the physical mechanism of the pumping cycle, a new fluid suction/discharge criterion was developed, which is helpful for the understanding of the operating range of the hearting power and the design verification. The high speed data acquisition system was used to detect the thermal hydraulics of the heat driven pump. It is shown that a full cycle can be subdivided into a short liquid suction, a boiling and fluid discharge stage, followed by a pressure decrease stage. The circulation flow rate is small and can be estimated by the energy conservation equation. Higher heating power can shorten the cycle period. Even though the wall temperatures are oscillating with small amplitudes, such temperatures are mainly relied on the saturated temperature of the working fluid.

Acknowledgment

The work was supported by the Natural Science Foundation of Guangdong Province, China, with the contract number of 32700, and Science and Technology Bureau of Guangdong Province, China, with the contract number of 2003C33103.

References

[1] G.P. Peterson, An Introduction to Heat Pipes, Modeling, Testing and Applications, A Wiley-Interscience Publication, New York, 1994.
[2] T. Yamamoto, Y. Takamura, M. Katsuta, Study of heat driven pump, J. Fuel Soc. Jpn. 59 (644) (1980) 1016–1024.
[3] T. Yamamoto, Y. Takamura, M. Katsuta, Study of heat driven pump, J. Fuel Soc. Jpn. 12 (1) (1982) 19–24.
[4] Y. Takamura, T. Yamamoto, M. Katsuta, Proposal heat driven pump for heat device, in: Proceedings of the International Conference on Energy and Environment, May 1995, p. 538.
[5] Y. Takamura, T. Yamamoto, S. Matsumoto, M. Katsuta, Development of downward heat pipe using principle of heat driven pump, in: K. Chen, G. Sarlos, T.W. Tong (Eds.), Proceedings of the International Conference on Energy and Environment, Shanghai, China, May 1998.
[6] J.L. Xu, X.Y. Huang, T.N. Wong, Study on heat driven pump. Part 1—experimental measurements, Int. J. Heat Mass Transfer 46 (2003) 3329–3335.
[7] J.L. Xu, T.N. Wong, X.Y. Huang, Study on heat driven pump. Part 2—mathematic modeling, Int. J. Heat Mass Transfer 46 (2003) 3336–3347.
[8] S.M. Yang, W.Q. Tao, Heat Transfer, Textbook Series for 21st Century, Higher Education Press, Third Version (in Chinese).